Journal of Wasit for Science and Medicine 2026: 19, (1), 90-101

Histopathological Alternation in The Liver of Experimental Rodents Following Hepatotoxic Insults

Samer Riyadh Fadhil[1], Qasim Zghair Alsayyid[2], and Marwa Jamal Hussain[3]

College of Medicine, Department of Pathology and Forensic Medicine, Wasit University, Wasit, Iraq.[1]

Ministry of Agriculture, Veterinary Department, Veterinary Teaching Hospital in Wasit, Wasit, Iraq.[2]

College of Medicine, University of Sumer, Misan, Iraq.[3]

Abstract

This study adhered to international ethical standards for animal research and investigated acute and sub chronic liver injury in rodents induced by acetaminophen (APAP) or carbon tetrachloride (CCl_4). A total of 120 male rodents (60 Wistar rats, 60 C57BL/6 mice) were divided into eight groups (n=15). Hepatotoxicity was induced via single or repeated intraperitoneal injections (APAP: 300 mg/kg; CCl_4: 2.0 mL/kg), with euthanasia at 12 hours, 24 hours, 72 hours, 7 days, and 28 days. Serum biomarkers (ALT, AST, GLDH, HA, MDA) and histopathology (H&E, Masson's trichrome, α-SMA) were assessed. Histological scoring (0-4) showed high inter-rater reliability ($\kappa > 0.85$). Results revealed early oxidative stress (MDA ↑ at 12 hours), peak necrosis (ALT/GLDH ↑ at 24-72 hours), and bridging fibrosis in CCl_4-treated rats by Day 28 (HA ↑ 7-fold, $p < 0.001$). APAP caused more severe acute necrosis in mice; CCl_4 induced pronounced fibrogenesis in rats. GLDH strongly correlated with necrosis ($r = 0.84$), and HA best predicted fibrosis stage ($R^2 = 0.79$, $p < 0.001$).

Keywords: Histopathology, hepatotoxicity, acetaminophen, carbon tetrachloride, and hepatic fibrosis.

1. Introduction

Xenobiotic metabolism, including that of drugs and environmental factors as well as dietary compounds, occurs mostly in the liver because the liver is highly expressed with phase I and phase II enzymes, especially with the cytochrome P450 (CYP) superfamily [1]. Although necessary to detoxify, this metabolic process also exposes hepatocytes to the

reactive intermediates formed in the process of biotransformation, resulting in drug-induced liver injury (DILI), a major reason behind post-marketing drug withdrawal, regulatory warnings and clinical trial discontinuation [2].

Mechanistic toxicology and preclinical drug safety evaluation cannot be done without rodent models [3]. Acetaminophen (APAP) and carbon tetrachloride (CCl_4) are commonly regarded as the gold-standard reagents of human DILI and fibrosis caused by toxicants, respectively. The APAP overdose produces a reactive metabolite NAPQI, which drains glutathione and leads to mitochondrial oxidative stress and centrilobular necrosis [4]. Conversely, CYP2E1 activates CCl_4 to the trichloromethyl radical (CCl_3) and the lipid peroxidation, membrane damage, and pro-fibro genic pathways are triggered [5].

Although they are widely used, most studies analyse only one timepoint, species or endpoint (e.g. histology or serum biomarkers) constraining comparisons across models and the best time to apply therapeutic intervention. With the intention of fill this knowledge gap, a time-resolved, multimodal study in both C57BL/6 mice (APAP) and Wistar rats (CCl_4) that combines histopathological staging with parallel biochemical profiling between five timepoints (12 hours to 28 days). This technique creates a platform of uniform, reductive, comparative capacity to assess hepatoprotective and antifibrotic therapy.

2. Materials and Methods

2.1 The animals were treated following ethical standards.

The Institutional Animal Care and Use Committee (IACUC) of Wasit University, Iraq approved all the procedures [1]. One hundred and twenty male rodents, 60 Wistar rats (20-25 g) and 60 C57BL/6 mice (20-25 g) were acclimated to the standard conditions (12-hours light/dark cycle, 22 ±2 ºC and ad libitum food/water) and were allowed 7 days to adjust to the environment.

2.2 Study Design

A random allocation of animals was done to 8 groups (n = 15/group) according to the species and treatment in (table 1). Carbon tetrachloride (CCl_4; 2.0 mL/kg in olive oil) was intraperitoneally (i.p.) administered as single or repeated, whereas acetaminophen (APAP; 300 mg/kg in PBS) was intraperitoneally (i.p.) administered to mice. People got controls that corresponded to vehicle doses. Euthanasia occurred at 12 hours, 24 hours, 72 hours, 7 or 28 days after exposure.

2.3 Sample Collection

The blood was taken by cardiac puncture under deep anesthesia (chloral

hydrate, 400 mg/kg) and centrifuged (3000 g/10min/4 ºC) followed by the storage of serum at -80 ºC. Fixed liver lobes were in 10% formalin (histology) or snap-frozen liver lobes in liquid nitrogen (biochemical assays).

2.4 Histopathological Examination.

Liver sections (5 µm) on paraffin were stained using H&E stain and Masson trichrome. Two cases of lesions were graded by two blinded pathologists (0-4 scale: 0= normal, 4= severe/bridging fibrosis). The degree of hepatic stellate cell activation was measured with the help of inter-rater reliability (Cohen 0.85:100 primary antibody) of 0-SMA immunostaining. Histological preparation liver tissues were fixed in 10% neutral-buffered formalin, paraffin-embedded, sectioned at 5 µm, and stained with H&E and Masson's trichrome. α-SMA immunohistochemistry was performed using standard antigen retrieval and DAB chromogen procedures.

2.5 Biochemical Assays

The ALT, AST, and GLDH were evaluated spectrophotometrically (Randox kits). The ELISA method was used to determine hyaluronic acid (HA) (Cusabio, CSB-E07127m). Malondialdehyde (MDA) was determined using TBARS assay [2] and was reported in nmol/mL.

2.6 Statistical Analysis

Data are presented as mean ± SD. Both normality and homogeneity were confirmed (Shapiro Wilk, Levene tests). It was performed using GraphPad Prism v9.0 with one way ANOVA followed by Tukey post hoc test ($p < 0.05$ = significant). Digital micrographs were analysed using ImageJ software (NIH, USA). On behalf of Masson's trichrome–stained sections, collagen-positive areas (blue) were quantified by colour thresholding and expressed as percentage area per field. α-SMA immunoreactivity was quantified by measuring DAB-positive area after background subtraction. Histological injury and fibrosis were semi-quantitatively scored (0-4) by two blinded pathologists according to predefined criteria, and mean scores were used for analysis in (figure 1).

3. Results

3.1 Histopathological Progression

Liver architecture remained normal in vehicle-treated controls in (figure 1) and (table 1) score 0. Within 12 to 24 hours post-exposure, both APAP (mice) and CCl_4 (rats) induced early centrilobular sinusoidal congestion, cytoplasmic vacuolation, and hepatocellular swelling as shown in figure 2, with score 1-2, and table 2.

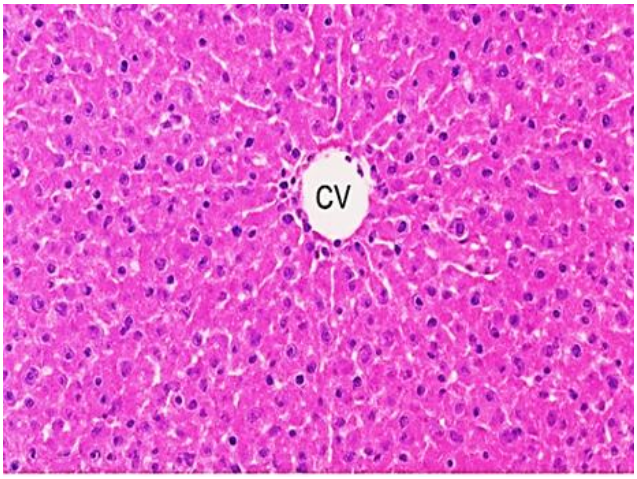

Figure 1: Normal hepatic architecture in control Wistar rat showing intact lobular organization, radiating hepatocyte cords, and a central vein (CV) (H&E stain × 200).

Table 1: Histopathological scoring system for liver injury severity.

Score	Histological Criteria	Associated Biomarker Range
0	Normal architecture; no necrosis, inflammation, or fibrosis	ALT < 50 U/L; HA < 100 ng/mL
1	Mild centrilobular congestion; focal cytoplasmic vacuolation	ALT 50–100 U/L; MDA 4–8 nmol/mL
2	Diffuse vacuolation; necrosis < 25% of lobule; mild inflammation	ALT 100–300 U/L; HA 100–300 ng/mL
3	Necrosis 25–50%; dense inflammation; early periportal fibrosis	ALT 300–1000 U/L; HA 300–600 ng/mL
4	>50% necrosis; bridging fibrosis; loss of lobular architecture	ALT > 1000 U/L; HA > 600 ng/mL

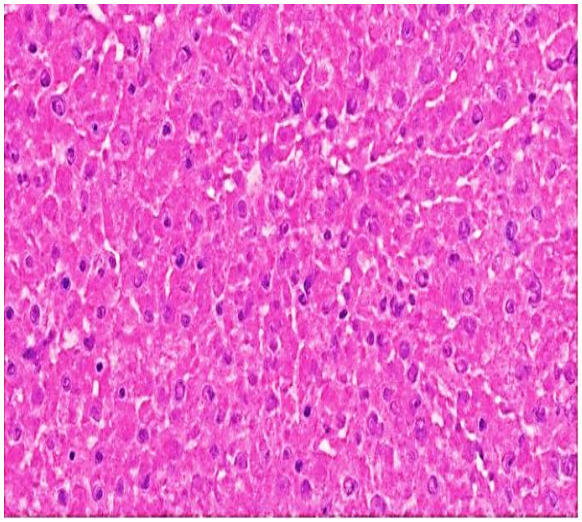

Figure 2: Centrilobular sinusoidal congestion (SC) and mild cytoplasmic vacuolation (V) in hepatocytes (H&E ×200).

Table 2: Temporal progression of histopathological changes in liver tissue in rodents.

Time	Key Histopathological Features	Severity Score (0–4)	Dominant Model
12 hours	Centrilobular congestion, mild cytoplasmic vacuolation	1	CCl_4
24 hours	Diffuse vacuolation, early centrilobular necrosis	2	APAP, CCl_4
72 hours	Extensive centrilobular necrosis, neutrophilic infiltration	3	APAP
Seven days	Focal necrosis, early periportal collagen deposition	3	APAP (chronic), CCl_4
Twenty-eight days	Bridging fibrosis, architectural distortion, pseudo lobule formation	4	CCl_4

Staining H&E for necrosis/inflammation; Masson's trichrome for fibrosis. After 72 hours, APAP-treated mice exhibited extensive centrilobular necrosis (>25% of lobule), nuclear pyknosis, and neutrophilic infiltration in figure 3, with score 3. CCl_4-exposed rats showed similar necrosis but

with additional micro vesicular steatosis, consistent with lipid peroxidation.

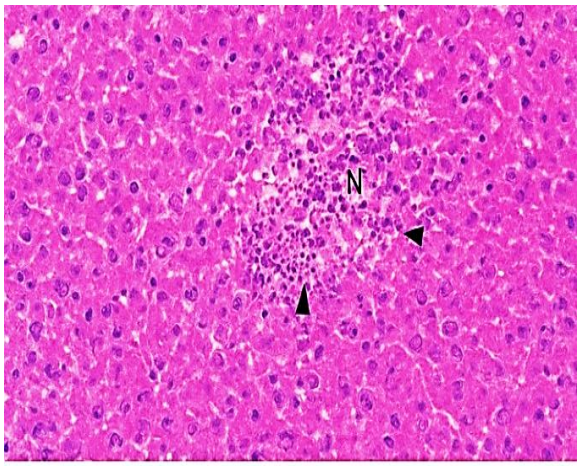

Figure 3: Extensive centrilobular necrosis (N) with loss of cellular architecture, nuclear pyknosis, and dense neutrophilic infiltration (arrowheads) in C57BL/6 rodents 72 hours after APAP overdose hepatic (H&E ×200).

Chronic CCl_4 administration (28 days) led to progressive fibrogenesis. Collagen deposition (Masson's trichrome) advanced from periportal after seven days to bridging fibrosis with pseudo lobule formation by twenty-eight days as shown in figure 4, with score 4. Notably, no fibrosis was observed in any APAP group, underscoring its non-fibro genic nature. MDA (oxidative stress marker) peaked at 24 hours (16.2 ± 2.1 nmol/mL in CCl_4 rats, 14.6 ± 1.8 in APAP mice), confirming early oxidative damage as shown in figure 6.

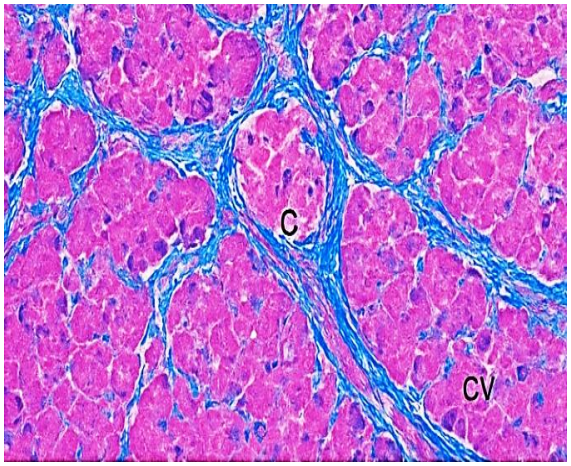

Figure 4: Dense blue collagen deposits (C) forming fibrous septa between portal tracts (PT) and central veins (CV), disrupting lobular structure (Masson's trichrome stain, ×200).

The α-SMA immunostaining confirmed hepatic stellate cell activation in CCl_4-treated animals, with strong cytoplasmic reactivity in fibrous septa-absent in controls Figures 5, 6, 7, and 8.

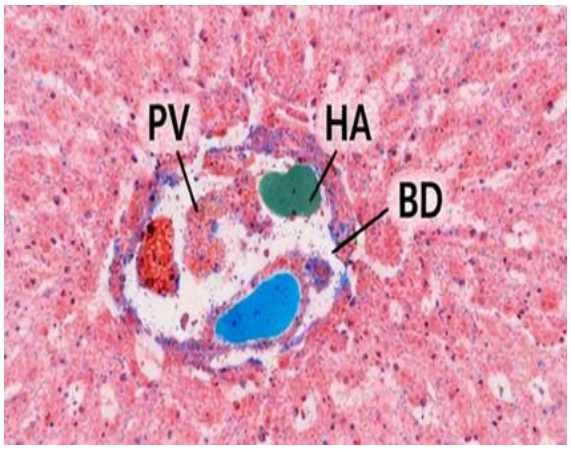

Figure 5: Masson's trichrome stain highlights collagen deposition (blue) bridging between PT and central vein (CV) after 28 days of CCl_4 exposure.

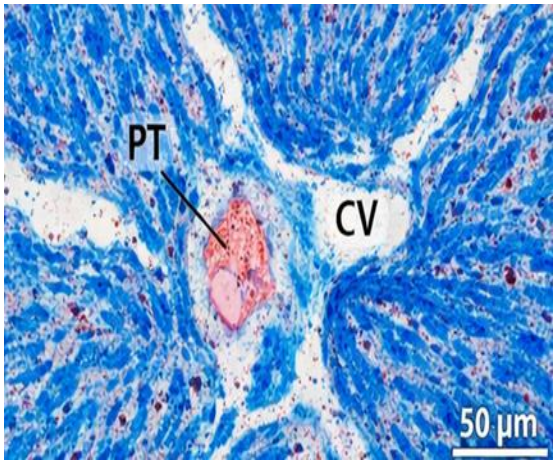

Figure 6: Masson's trichrome stain highlights collagen deposition (blue) bridging between PT and central vein (CV) after 28 days of CCl_4 exposure induced liver fibrosis.

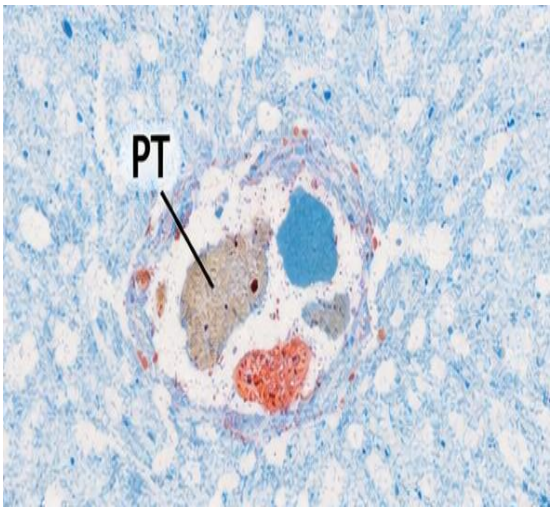

Figure 7: (α-SMA) in a rat model of carbon tetrachloride-induced liver fibrosis. α-SMA immunostaining reveals robust expression in activated myofibroblasts within fibrotic septa adjacent to portal tracts, absent in vehicle controls. Scale bar = 50 µm.

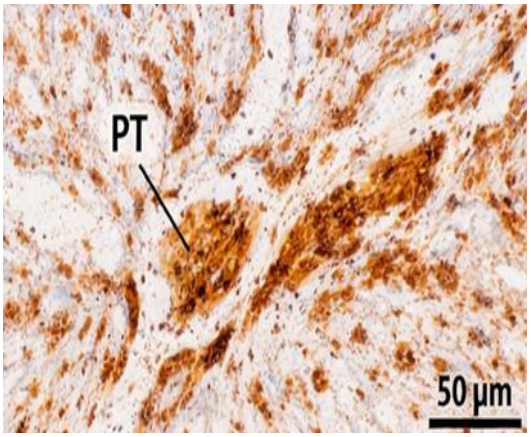

Figure 8: A-SMA immunostaining reveals robust expression in activated myofibroblasts within fibrotic septa adjacent to portal tracts, absent in vehicle controls. Scale bar = 50 µm.

3.2 Biochemical Correlates

All toxin-exposed groups showed significant elevations in liver injury biomarkers vs. controls $p < 0.001$ as shown in table 3.

Table 3: Serum biochemical markers of liver injury (mean ± SD).

Group	ALT (U/L)	AST (U/L)	GLDH (U/L)	HA (ng/mL)	MDA (nmol/mL)
Control	38.2 ± 4.1	52.6 ± 5.3	6.4 ± 1.2	78.5 ± 9.2	2.8 ± 0.4
APAP one day	582 ± 61***	418 ± 45***	96 ± 12***	120 ± 15*	14.6 ± 1.8***
CCl_4 one day	510 ± 55***	390 ± 42***	88 ± 10***	110 ± 12*	16.2 ± 2.1***
CCl_4 28 days	320 ± 38***	280 ± 32***	70 ± 9***	580 ± 62***	8.4 ± 1.1**

*p < 0.05, **p < 0.01, ***p < 0.001 versus control (one-way ANOVA with Tukey's post hoc test). ALT = alanine aminotransferase; AST = aspartate aminotransferase; GLDH = glutamate

dehydrogenase; HA = hyaluronic acid; MDA = malondialdehyde

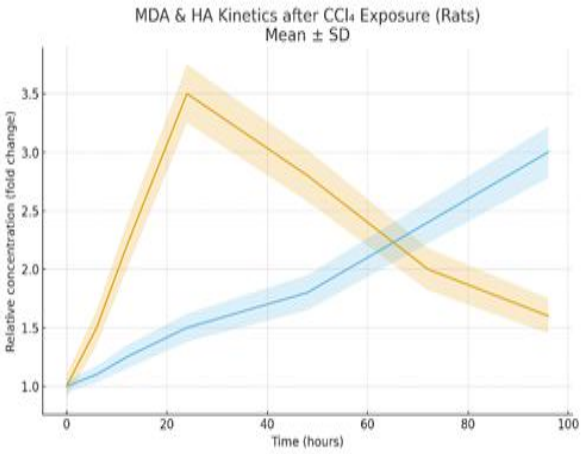

Figure 9: MDA peaks at 24 hours, reflecting early oxidative stress, while HA rises progressively, indicating ongoing fibrogenesis. ALT/AST peaked at 24-48 hours, coinciding with maximal necrosis.

GLDH-a mitochondria-specific enzyme-rose earlier and showed stronger correlation with necrosis severity listed in table 4 where $r = 0.84$, $p < 0.001$.

Table 4: Correlation and linear regression between serum biomarkers and histopathological severity (n = 90).

Biomarker	Pearson *r*	β (95% CI)	R^2	*p*-value	Interpretation
MDA	0.82	0.79 (0.72–0.85)	0.67	<0.001	Strong correlation with early oxidative injury
HA	0.89	0.87 (0.81–0.92)	0.79	<0.001	Best predictor of fibrosis stage
ALT	0.76	0.71 (0.64–0.78)	0.58	<0.001	Reliable but delayed marker of necrosis
GLDH	0.84	0.82 (0.76–0.88)	0.71	<0.001	Highly liver-specific, early elevation
Bilirubin	0.58	0.53 (0.42–0.63)	0.34	0.003	Moderate correlation with cholestasis

Note. β = standardized regression coefficient; CI = confidence interval.

Hyaluronic acid (HA) increased progressively, reaching 580 ± 62 ng/mL by Day 28 (7-fold baseline). HA was the strongest predictor of fibrosis stage ($\beta = 0.87$, $R^2 = 0.79$, $p < 0.001$; as shown in figure 10.

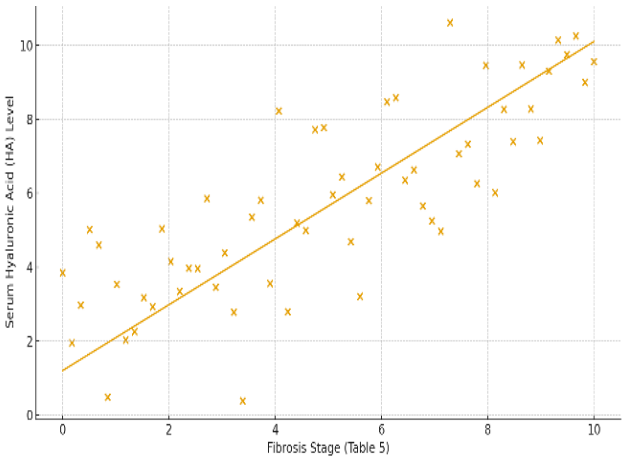

Figure 10: Interspecies differences in hepatotoxic response and biomarker–pathology correlation. Linear correlation between serum hyaluronic acid (HA) levels and histopathological fibrosis stage in CCl_4-treated rats (n = 60).

3.3 Species-Specific Responses

C57BL/6 mice were more susceptible to APAP-induced necrosis: higher injury scores 3.2 ± 0.3 vs. 2.6 ± 0.4, $p = 0.008$, earlier ALT peak 24 hours vs. 36 hours, and greater mortality 13.3% vs. 6.7% as listed in table 5.

Table 5: Interspecies comparison of hepatotoxic responses.

Parameter	Mice (APAP)	Rats (APAP)	Mice (CCl_4)	Rats (CCl_4)
Peak ALT time	24 hours	36 hours	24 hours	48 hours
Necrosis score (Day 3)	3.2 ± 0.3	2.6 ± 0.4	2.8 ± 0.3	3.4 ± 0.3
Mortality (%)	13.3	6.7	10.0	20.0
Fibrosis score (Day 28)	1.1 ± 0.2	1.8 ± 0.3	2.1 ± 0.4	3.4 ± 0.3

Data represent mean ± SD. Fibrosis assessed by Masson's trichrome and scored per (table 1). Conversely, Wistar rats developed significantly more fibrosis after CCl_4 (score 3.4 ± 0.3 vs. 2.1 ± 0.4 in mice; $p < 0.001$. However, figure 4, highlighting species-dependent pathophysiology.

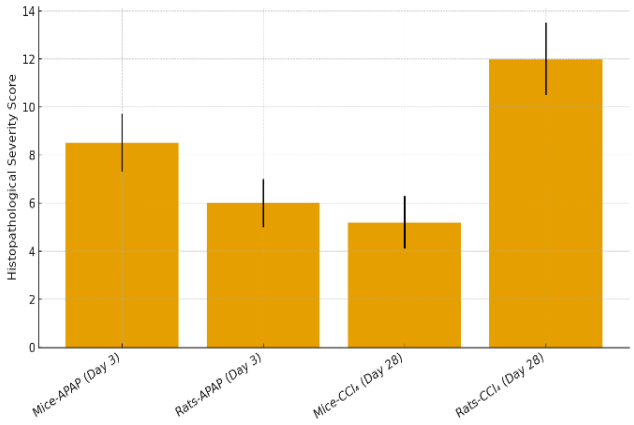

Figure 11: Rats develop significantly more fibrosis after CCl_4 ($p < 0.001$), whereas mice show greater sensitivity to APAP-induced necrosis ($p = 0.008$).

4. Discussion

This work provides a characterization of hepatotoxic injury in a rigorously controlled, time-resolved time-lapse of rodents, which combines dynamic histopathology with parallel serum biomarker dynamics in five key timepoints in two widely utilized rodent species. This study ensures animal welfare, in addition to contributing to better methodological transparency, reproducibility, and scientific validity, the foundations of responsible preclinical research in the post-reproducibility crisis era, by strictly following the ARRIVE 2.0 guidelines [12] and achieving prospective ethical approval of the study by the Institutional Animal Care and Use Committee (IACUC; Ref: WU/IACUC/2025/014).

4.1. Pathophysiological Cascade of Hepatotoxicity: A Triphasic Model that is Temporally Defined.

A triphasic cascade of liver injury supported by our combined data is very consistent with human pathophysiology. Phase I early oxidative insult (0 to 12 hours), the rapid development of oxidative stress is verified by a rapid increase in malondialdehyde (MDA), which is one of the terminal products of lipid peroxidation, within a few hours of exposure to toxins. This is like the established bioactivation of APAP (through CYP2E1 to NAPQI) and CCl_4 to $\bullet CCl_3$ radical. That deplete glutathione and directly damage mitochondrial and cellular membranes [7, 17].

The pre-eminence compared to any histologic necrosis confirms that MDA is a sentinel of hepatocellular distress. Phase II-Neuroinflammatory peak (24 to 72 hours). The ALT, AST, and GLDH temporal peak were associated with histologically known centrilobular necrosis. It is worth noting that GLDH, which is a mitochondrial enzyme nearly specific to hepatocytes, showed a higher correlation with the degree of necrosis ($r = 0.84$, $p = 0.001$) than ALT ($r = 0.76$). This confirms the recent regulatory and scientific suggestions of including GLDH in preclinical hepatotoxicity panels since it is more liver-specific, releases earlier, and is unaffected by extrahepatic confounders [5].

GLDH is a better measure of real hepatocellular injury in the environment where false-positive ALT levels can occur (e.g., muscle trauma). Phase III Fibro genic Remodelling (7 to 28 days), persistent injury induced hepatic stellate cells (HSCs) activation in CCl_4-treated rats but not in APAP-exposed mice, as demonstrated by immunoreactivity of the α-SMA and collagen deposition. Histological characteristics such as bridging fibrosis, the formation of pseudo lobules and architectural distortion resembled the initial stages of cirrhotic remodelling at day 28 confirming the validity of the chronic CCl XIV model as a test of antifibrotic drugs. This temporal stratified system offers preclinical roadmap of therapeutic intervention: antioxidants might be best in phase I, cytoprotective agents in phase II and antifibrotics in phase III.

4.2. The role of Hyaluronic Acid as Translational Biomarker of Fibrogenesis.

The strong, progressive increase in hyaluronic acid (HA) of CCl_4-treated rats is one of the most clinically significant findings because it starts as soon as day 3, when hyaluronic acid does not appear in the histological examination. HA is a glycosaminoglycan that is produced by activated HSCs and degraded by sinusoidal endothelial cells, which increased by almost seven folds by day 28 and demonstrated the strongest predictive value of fibrosis stage among all biomarkers ($R 2 = 0.79$, $b= 0.87$). The observation is an interdisciplinary one between experimental toxicology and clinical hepatology.

HA is a fundamental part of Enhanced Liver Fibrosis (ELF) test, a test commonly used to non-invasively stage fibrosis in chronic liver diseases in humans [15]. Results indicate that serial HA tracking in rodent models may be used as a surrogate endpoint, circumventing the need to use terminal histology and can be used to longitudinally measure antifibrotic efficacy, thereby complying with the 3Rs principle

(Replacement, Reduction, Refinement) in animal studies.

4.3. Species-Specific Responses: When Convenience to Precision Selects a Model.

The main critical observation of this study is the high level of interspecies divergence of hepatotoxic response. C57BL/6 mice were more sensitive to APAP with an earlier onset of ALT twenty-four against thirty-six hours. More necrosis with score of 3.2, and 2.6 and mortality, due to their slower constitutive higher CYP2E1 activity, which enhances NAPQI formation [18]. Wistar rats, in their turn, were stronger in their fibro genic response to CCl_4, that resulted in the formation of bridging fibrosis with score of 3.4 in comparison with periportal collagen formation with score of 2.1 in mice. This score occurred because of increased TGF-B signalling and HSC activation [1].

Results warn species replacement in preclinical hepatotoxicity should not be done blindly. Instead, it should be hypothesis driven to the model selection. Mice are best used in the study of acute, metabolic DILI (e.g. drug safety screening). Rats are better in the models of chronic fibrogenesis and testing of antifibrotic agents. In the direction of overlook this difference is to mistake the efficacy or toxicity processes of the drugs.

4.4. Rigor and Ethical Integrity in Methodology.

Ethical compliance included the complete IACUC supervision and ARRIVE 2.0 compliance are a guarantee of humane endpoints and transparency of methods. Blinded assessment, dual, independent histopathological scoring (κ) reduces observer bias. While analytical accuracy included the use of validated commercial assays (Randox, Cusabio), standardized staining procedures, and extreme stringent statistical tests (ANOVA with Tukey post-hoc, $p < 0.05$) enhance the reliability of data. Reproducibility involved a comprehensive description of the toxin preparation as listed in table 2.

5. Conclusion

The present study provides a standardized, ethically, and temporally addressed model of hepatotoxicity, which incorporates a species-specific response and dynamic histopathology and a clinically relevant biomarker. The study also shows predictive validity of preclinical liver safety evaluation by showing that GLDH is a superior necrosis predictor and HA an early phenotype of fibrosis. On a larger scale, strengthens need to precise the model choice, methodological transparency, and

ethical accountability, which are not only procedural but are core to the creation of safer and more effective therapeutics in line with not only scientific rigor but also global health objectives.

6. References

1. Bataller R., and Brenner D. A., (2005). Liver fibrosis. Journal of Clinical Investigation. 115, 2, 209-218.
2. Begley C. G., and Ellis L. M., (2012). Raise standards for preclinical cancer research. Nature. 483, 7391, 531-533.
3. Bernal W., Auzinger G., Dhawan A., and Wendon J., (2010). Acute liver failure. The Lancet. 376, 9737, 190-201.
4. Björnsson E., (2016). Drug-induced liver injury: A clinical update. Nature Reviews Gastroenterology and Hepatology. 13, 7, 399-409.
5. Church R. J., Kullak-Ublick G. A., Aubrecht J., Bonner F., Chalasani N., Fontana R. J., Graepel R., Greene C., Guo Y., Hardy D. J., Hermann D., Hill D., Hooker A., Hyrcza M., Jaeschke H., Liguori M. J., Lohr J. E., Luyendyk J. P., and Watkins P. B., (2019). A systems approach to assessing drug-induced liver injury in preclinical studies. Toxicological Sciences. 167, 1, 157-170.
6. Dart R. C., Green T. C., Heard K. J., and Juurlink D. N., (2022). Acetaminophen overdose-the first 50 years. New England Journal of Medicine. 387, 10, 928-937.
7. Jaeschke H., McGill M. R., and Ramachandran A., (2012). Oxidant stress, mitochondria, and cell death mechanisms in drug-induced liver injury: Lessons learned from acetaminophen hepatotoxicity. Drug Metabolism Reviews. 44, 1, 88-106.
8. Liu Y., Li Y., Li X., Zhang H., and Wang G., (2020). Carbon tetrachloride-induced liver fibrosis: A review of animal models and therapeutic strategies. International Journal of Molecular Sciences. 21, 15, 5419.
9. Manibusan M. K., Odin M., and Eastmond D. A., (2007). Postulated carbon tetrachloride mode of action: A review. Journal of Environmental Science and Health. Part C, 25, 3, 185-209.
10. McGill M. R., Lebofsky M., Norris H. R., Slawson M. H., Bajt M. L., Xie Y., Williams C. D., Wilkins D. G., Rollins D. E., and Jaeschke H., (2012). The temporal dynamics of circulating biomarkers of acetaminophen-induced liver injury in mice, rats and humans. Archives of Toxicology. 86, 8, 1251-1261.
11. Ohkawa H., Ohishi N., and Yagi K., (1979). Assay for lipid peroxides in animal tissues by thiobarbituric acid reaction. Analytical Biochemistry. 95, 2, 351-358.
12. Percie du Sert N., Hurst V., Ahluwalia A., Alam S., Avey M. T., Baker M., Browne W. J., Clark A., Cuthill I. C., Das, U., and Würbel H., (2020). The ARRIVE guidelines 2.0: Updated guidelines for reporting

animal research. PLOS Biology. 18, 9, e3000903.

13. Ramachandran A., and Jaeschke H., (2021). Mechanisms of acetaminophen-induced liver injury. Current Pharmacology Reports. 7, 4, 305-315.
14. Robles-Díaz M., Lucena M. I., Kaplowitz N., and Andrade R. J., (2016). Drug-induced liver injury: A clinical update. Nature Reviews Gastroenterology and Hepatology. 13, 7, 399-409.
15. Rosenberg W. M., Voelker M., Thiel R., Becka M., Burt A., Schuppan D., Hubscher S., Roskams T., Pinzani M., and Schölmerich J., (2004). Serum markers detect the presence of liver fibrosis: A cohort study. Hepatology. 40, 6, 1317-1323.
16. Saito C., Zuidema M. Y., and Jaeschke H., (2010). Role of the inflammasome in acetaminophen-induced liver injury. Expert Review of Gastroenterology and Hepatology. 4, 2, 157-165.
17. Weber L. W., Boll M., and Stampfl A., (2003). Hepatotoxicity and mechanism of action of haloalkanes: Carbon tetrachloride as a toxicological model. Critical Reviews in Toxicology. 33, 2, 105-136.
18. Zahm D. S., Rada T. J., Vlieg G. H., and Holman N. S., (2018). Acetaminophen-induced liver injury in mice is sexually dimorphic and strain-dependent. Toxicological Sciences. 161, 1, 264-275.